Biochar
https://doi.org/10.1007/s42773-020-00079-7

ORIGINAL RESEARCH

Removal of sodium diclofenac from aqueous solutions by rice hull biochar

Judilyn Q. Filipinas[1,2] · Kim Katrina P. Rivera[3] · Dennis C. Ong[4] · Sheila Mae B. Pingul-Ong[4] · Ralf Ruffel M. Abarca[1] · Mark Daniel G. de Luna[1,3]

Received: 27 June 2020 / Accepted: 24 November 2020

Abstract

Diclofenac is an ecotoxic pharmaceutical compound affecting both aquatic and terrestrial ecosystems even at low concentrations. In this study, batch adsorption experiments were conducted to remove sodium diclofenac (SD) from aqueous solutions using rice hull biochar (RHB) adsorbents. Higher SD removals were obtained with increasing initial SD concentration, RHB dosage, contact time, and decreasing initial pH. Isotherm studies revealed that Langmuir isotherm best fitted the experimental data with the highest coefficient of determination for both pH 2 ($R^2 = 0.9827$) and pH 7 ($R^2 = 0.9460$). For kinetic studies, the pseudo second-order model gave $R^2 = 0.9999$ for both pH 2 and pH 7. SD removals reached up to 97% at pH 2 and up to 80% at pH 7. Higher SD removals were achieved at solution pH lower than the adsorbent pH_{pzc} since electrostatic repulsion was eliminated. Fourier-transform infrared analysis showed the major involvement of C=O in the adsorption process. This study demonstrated the potential of using agricultural residues such as rice hulls for the treatment of wastewater contaminated with pharmaceutical compounds.

Graphic abstract

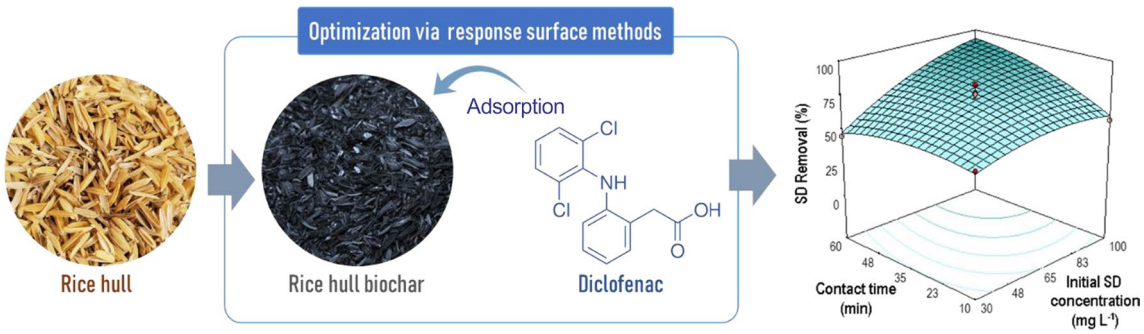

Keywords Adsorption · Biochar · Isotherm · Kinetics · Rice hull · Sodium diclofenac

Nomenclature

C_0 Initial SD concentration, mg L^{-1}
C Final SD concentration, mg L^{-1}
Q Equilibrium adsorption capacity, mg g^{-1}
q_m Maximum adsorption capacity, mg g^{-1}
b Energy of adsorption, L mg^{-1}
C_e Equilibrium concentration of the adsorbate, mg L^{-1}

✉ Dennis C. Ong
dcong@up.edu.ph

✉ Mark Daniel G. de Luna
mgdeluna@up.edu.ph

[1] Environmental Engineering Program, National Graduate School of Engineering, University of the Philippines Diliman, 1101 Quezon City, Philippines

[2] Department of Chemical Engineering, Mindanao State University Main Campus, Marawi City, Lanao del Sur, Philippines

[3] Department of Chemical Engineering, University of the Philippines Diliman, 1101 Quezon City, Philippines

[4] School of Technology, University of the Philippines Visayas, Miagao, 5023 Iloilo, Philippines

Published online: 11 January 2021

R_L Separation factor or equilibrium parameter
K_f Freundlich capacity factor, ($mg^{1-1/n}\ L^{1/n}\ g^{-1}$)
$1/n$ Intensity parameter
β Constant related to heat of sorption, J mol^{-1}
α Temkin isotherm equilibrium binding constant, L g^{-1}
q_t Amount of adsorbate at contact time t, mg g^{-1}
k_1 Pseudo-first-order rate constant, min^{-1}
k_2 Pseudo-second-order rate constant, g mg $^{-1}$ min^{-1}
k_{id} Intraparticle diffusion rate constant, mg g^{-1} $min^{-0.5}$

1 Introduction

Pharmaceuticals and personal care products (PPCPs) are emerging contaminants that have been a cause for concern in recent years (Hu et al. 2011). Extensive use of PPCPs, such as analgesics, antibiotics, contraceptives, lipid regulators, insect repellents, sunscreens, lotions, soaps, toothpaste, detergents, fragrances, and skin, hair, and dental care products, both in medical and veterinary practice has resulted in their presence in unaltered form in surface waters (Martínez et al. 2011; Liu and Wong 2013), since these persistent compounds are not removed completely by sewage treatment plants (STPs) and other conventional treatment methods (Gotostos et al. 2014). When these compounds are released into recipient waters, they can be bioaccumulated and, therefore, may present potential risks to human health and aquatic organisms (Sotelo et al. 2012).

Among the pharmaceutical substances that reach the aquatic environments via industrial effluents and human use, sodium diclofenac (SD) is the most widely detected (Wu et al. 2019). Chemically known as sodium 2-[(2,6-dichlorophenyl) amino] phenyl] acetate, SD is among the most extensively-used nonsteroidal anti-inflammatory drugs (NSAIDs) (Ensano et al. 2017). In fact, this drug is widely used to treat livestock especially across the Indian subcontinent (Green et al. 2004). The global consumption of diclofenac is estimated to be 940 tons per year, with detection concentration in surface waters, groundwaters, and even in drinking waters in the range of ng L^{-1} to µg L^{-1} in the last years (Malefane et al. 2019). Extensive studies on SD metabolism in humans and animals have been conducted (Fei et al. 2006; Tiwari et al. 2015), and it was discovered that after ingestion, unchanged diclofenac, together with its hydroxylated metabolites, are excreted by the body through urine and feces (Stülten et al. 2008). These compounds enter wastewater treatment plants (WWTP) where the removal percentage of SD typically ranges from 21% to 40% during the treatment processes (de Luna et al. 2017).

The adverse effects of these pharmaceutical compounds, such as SD, which has been proven to be ecotoxic and affects both aquatic and terrestrial ecosystems (Oaks et al. 2004), have led to strict regulations that require the elimination of pharmaceutical residues from industrial wastewaters. PPCPs are commonly removed from wastewaters by membrane filtration (de Luna et al. 2019), advanced oxidation processes (Lin et al. 2016), photodegradation (Paragas et al. 2018), and adsorption (Abo El Naga et al. 2019). However, the large-scale application of these technologies is hindered by the high cost of installation. Among the various treatment systems for pharmaceutical wastewaters, adsorption is by far one of the most promising. In particular, the use of biochar as sorbent material addresses the high cost of commercially available activated carbon.

Biochar is a carbonaceous product of biomass thermal conversion under low-oxygen environment (Kim et al. 2020). It is the prime product of torrefaction at 200–300 °C, and a pyrolysis by-product at 300–600 °C (Genuino et al. 2018; Arriola et al. 2020). It is an organic-rich material that is effective in the adsorption of pharmaceuticals (Genuino et al. 2017). Availability, abundance, low cost, and the renewable nature of the adsorbent material, along with the simple preparation method and ease of process operations, are among the advantages of this technology (Antunes et al. 2012; Ifthikar et al. 2017). Several agricultural wastes and other materials like municipal solid wastes have been used as biochar precursors for decontaminating industrial/domestic wastewater (Sumalinog et al. 2018). A particularly abundant agricultural waste that can be used for biochar production is rice hull, which is the residue obtained from the rice milling process. While rice hulls have been used as fuel in boiler furnaces of various industries to produce steam, these agricultural residues have limited or no practical use in the Philippines. The annual generation of rice hulls exceeds 140 million tons worldwide, 96% of which comes from developing countries (Kalderis et al. 2008). Since the rice industry is expected to continue for a long time, with predicted total rice consumption at 450 million tons by 2020 (milled basis) (Lim et al. 2012), the availability of rice by-products will remain high. Thus, utilization of rice hull as adsorbent can add value to this waste material and significantly contribute to effective waste management. Several studies have reported on the application of rice hull biochar (RHB) for dye (Khan et al. 2020) and heavy metals (Han et al. 2020) removal. However, the application of RHB for the removal of SD from water matrices has not yet been fully explored.

Biochar adsorbents derived from rice hulls were previously prepared in various researches at temperatures ranging from 270 °C to 700 °C (Leksungnoen et al. 2019; Shi et al. 2019), with some studies utilizing a variety of modifications, such as microwave-assisted pyrolysis, steam activation, acid activation, alkaline activation, CO_2 activation and electrochemical modification (Wang et al. 2020b). However, rice hull adsorbents may also be prepared through torrefaction at lower temperatures (200–300 °C) (Arpia et al. 2021) and

without modifications or use of chemical activating agents (de Luna et al. 2013). This process conforms with the essential advantages of using biochar as adsorbents which are low cost and compatibility with green manufacturing (Wang et al. 2018). Compared with biochar modification processes that require high activation temperatures and chemical activating agents, the process used in this study is more economical, requires low energy consumption, and is environment friendly.

The study aims to determine the applicability of RHB in removing SD from aqueous solutions. Parametric studies were done to determine the effects of operating parameters such as initial SD concentration, RHB dosage, initial solution pH, and contact time on SD removal. Box–Behnken design (BBD) was used to determine the optimum conditions of these parameters. Isotherm and kinetic studies were employed to identify the best-fitting models, as well as the dominant mechanism of the adsorption process.

2 Materials and methods

2.1 Preparation of SD aqueous solutions and rice hull adsorbents

All chemicals used in this study were of analytical grade. A synthetic SD stock solution (500 mg L^{-1}) was prepared by dissolving diclofenac sodium salt ($C_{14}H_{10}Cl_2NNaO_2$, 99%, Sigma-Aldrich) in distilled water. Working SD solutions were prepared by diluting the stock solution with distilled water.

Rice hulls were obtained from a rice mill in Muñoz, Nueva Ecija, Philippines. The rice hulls were washed thoroughly with distilled water to remove particles and water-soluble impurities. The washed hulls were dried in an oven at 100 °C for 30 min and pulverized in a Thomas-Wiley laboratory mill. The powdered hulls were sieved to obtain particles that were 300–500 µm in size and severely torrefied in an oven at 350 °C for 1 h. The RHB powder was then stored in clean and dry containers.

2.2 Analytical methods

The elemental compositions of raw rice hulls (RRH) and RHB were examined by energy dispersive X-ray analysis (EDX, TM-1000, Hitachi). The functional groups involved in SD adsorption were analyzed by Fourier-transform infrared (FTIR) spectroscopy (Nicolet 6700, Thermo Scientific). The point-of-zero charge (pH_{pzc}) was determined by mass titration method that used increasing amounts of RHB added to water to obtain suspensions of 0.01, 0.1, 1, 5, 10, and 20% by weight. These samples were agitated for 24 h and then filtered. The final pH of each suspension was measured after 24 h of contact time for which the value of pH equilibrium was reached. This value was approximately equal to the adsorbent pH_{pzc}.

Sample SD concentrations were determined following the study by Matin et al. (2005). SD-containing samples (2 mL) were combined with 1 mL concentrated nitric acid (HNO_3 63% w/v, Merck) to produce a yellowish compound diluted to 10 mL with distilled water. The absorbance of the resulting solution was read at maximum wavelength (λ_{max}) of 365 nm using a UV–Vis spectrophotometer (Model UV 1601, Shimadzu). Diclofenac removal was computed using the following equation:

$$\text{SD Removal } (\%) = \frac{C_0 - C}{C_0} \times 100. \tag{1}$$

2.3 Batch adsorption experiments: optimization, isotherm, and kinetic studies

Erlenmeyer flasks containing 20 mL samples of varying initial SD concentrations, RHB dosage, initial pH, and contact time were agitated using a magnetic stirrer at 300 rpm and 25 °C. The pH of the solution was adjusted with 0.1 M sodium hydroxide (NaOH 99%, Merck) and 0.1 M hydrochloric acid (HCl 99%, Merck). Box–Behnken design with three levels was used to optimize process parameters, namely initial SD concentration (30, 65, 100 mg L^{-1}), RHB dosage (0.1, 0.3, 0.5 g), initial pH (2, 5.5, 9), and contact time (10, 35, 60 min). Adsorption experiments were carried out at optimum conditions. For the isotherm study, SD solutions of different initial SD concentrations (20, 40, 60, 80, and 100 mg L^{-1}) were prepared at pH 2 and pH 7. Kinetic studies were conducted at varying durations (10, 20, 30, 40, 50, and 60 min). All the experiments were performed in triplicates. The adsorption capacity (Q) was computed using the following equation:

$$Q = \frac{\left(C_o - C\right) \text{ volume of solution}}{\text{mass of adsorbent}}. \tag{2}$$

3 Results and discussion

3.1 Adsorbent characterization

Raw rice hulls contain cellulose, hemicellulose, lignin, extractives, water and mineral ash. The mineral content include oxides of silicon, potassium, magnesium, iron, aluminum, and calcium (Nakbanpote et al. 2000). Figure 1 shows that RRH was composed mainly of carbon (16.53 wt%), oxygen (40.51 wt%), and silicon (42.96 wt%). Similar findings were previously reported (Souza et al. 2002). After severe torrefaction,

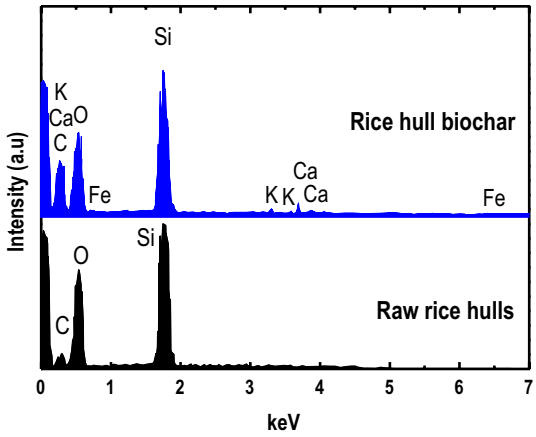

Fig. 1 EDX atomic composition of raw rice hulls (RRH) and rice hull biochar (RHB)

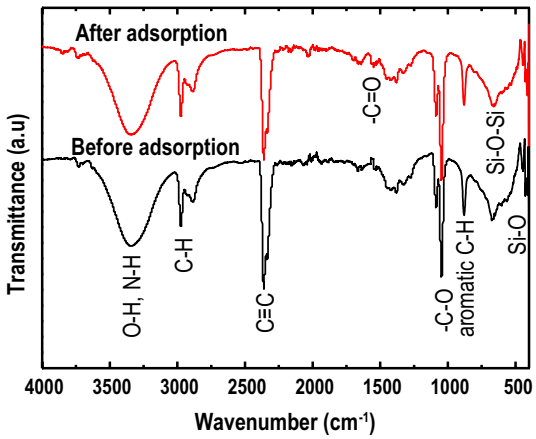

Fig. 2 FTIR spectra of RHB before and after adsorption

other elements from the mineral ash, such as potassium, calcium, and iron, were liberated and exposed. In addition to this, the atomic composition of carbon significantly increased from 25.3% to 40.48% after torrefaction, thus making RHB a more effective adsorbent compared to RRH (Nakbanpote et al. 2000; Wang et al. 2001; Souza et al. 2002).

The results of the FTIR analysis of RHB before and after adsorption are shown in the FTIR spectra presented in Fig. 2. The broad peak at 3300–3400 cm^{-1} corresponds to the stretching of –OH groups due to SiOH and adsorbed water (de Luna et al. 2013). The peak at 3000 cm^{-1} and those at 2100–2400 cm^{-1} are attributed to C–H stretching and C≡C stretching, respectively. Indications of aromatic C–H and C–O stretching are seen in the peaks at 800–1000 cm^{-1} and 1000–1100 cm^{-1}, respectively (de Luna et al. 2013). Si–O bond stretching vibration is also observed in the peak at 700 cm^{-1} (Chen et al. 2012). In addition, the peak at 1700 cm^{-1}, which corresponds to C=O stretching vibrations, resulted in the largest shift to 1900 cm^{-1} after SD adsorption (Coates 2000; Jeon 2011). This indicates that the stretching of the C=O in the carbonyl or carboxyl groups participated the most in the SD adsorption process (Yu et al. 2013).

3.2 Optimization of the adsorption parameters

In this study, Box–Behnken design (BBD) was used to investigate the effects of important operating parameters in the removal of SD using RHB adsorbent, and to determine the optimum condition for SD adsorption. BBD is a type of response surface method (RSM) which is based on a three-level incomplete factorial design, and requires fewer runs compared to other RSM designs (de Luna et al. 2012). From Box–Behnken design, the highest SD removal was 97% using the following experimental conditions: initial SD concentration = 100 mg L^{-1}, solution pH = 2, RHB dosage = 0.3 g and contact time = 35 min (Table 1). In contrast, the lowest SD removal was 41% at initial SD concentration = 65 mg L^{-1}, pH = 9, RHB dosage = 0.1 g and contact time = 35 min. This is consistent with the findings on the effect of varying initial solution pH on SD removal.

The results of the analysis of variance (ANOVA) presented in Table 2 show that the response surface quadratic model obtained was significant, with model *F*-value at 9.93. This indicates that the model can explain most of the variations in the response (de Luna et al. 2015). The high coefficient of determination (R^2) of 0.9145 and an adjusted R^2 value of 0.8224 indicate that the quadratic model is reliable in predicting responses. Likewise, all main parameters (initial SD concentration, RHB dose, initial pH, and contact time) and the interactions between initial SD concentration and contact time were significant, with *p* values of less than 0.05. Three-dimensional (3D) response surface plot (Fig. 3) was generated using RSM to show the significant interaction effects between contact time and initial SD concentration. As observed, longer contact time and higher initial SD concentration resulted in higher SD removal. This is attributed to the increased interaction between SD molecules and the available binding sites on the RHB surface.

The quadratic model equation in terms of coded factors is expressed by the following equation:

$$\begin{aligned} Y =& 76.797 + 13.262X_1 + 6.999X_2 - 14.921X_3 + 6.899X_3 \\ &+ 5.655X_1X_2 + 5.037X_1X_3 + 9.311X_1X_4 + 2.816X_2X_3 \\ &- -4.000X_2X_4 + 1.379X_3X_4 6.914X_1^2 - 4.964X_2^2 \\ &- +0.452X_3^2 - 5.911X_4^2, \end{aligned} \quad (3)$$

where *Y* is the predicted response variable for SD removal and X_1, X_2, X_3 and X_4 correspond to the independent

Table 1 BBD for SD removal using RHB

Run	X_1: Initial SD conc (mg L^{-1})	X_2: RHB Dosage (mg)	X_3: Initial pH	X_4: Contact Time (min)	Actual SD removal (%)	Predicted SD removal (%)
1	30	100	5.50	35	50	48
2	100	100	5.50	35	71	63
3	30	500	5.50	35	42	51
4	100	500	5.50	35	86	89
5	65	300	2.00	10	80	79
6	65	300	9.00	10	41	46
7	65	300	2.00	60	93	90
8	65	300	9.00	60	60	62
9	65	300	5.50	35	83	75
10	65	300	5.50	35	70	75
11	30	300	5.50	10	55	51
12	100	300	5.50	10	57	59
13	30	300	5.50	60	45	46
14	100	300	5.50	60	85	91
15	65	100	2.00	35	74	81
16	65	500	2.00	35	91	89
17	65	100	9.00	35	41	45
18	65	500	9.00	35	70	65
19	65	300	5.50	35	77	75
20	65	300	5.50	35	83	75
21	30	300	2.00	35	82	81
22	100	300	2.00	35	97	98
23	30	300	9.00	35	45	41
24	100	300	9.00	35	81	78
25	65	100	5.50	10	52	52
26	65	500	5.50	10	76	74
27	65	100	5.50	60	76	74
28	65	500	5.50	60	84	80
29	65	300	5.50	35	72	81
30	65	300	5.50	35	76	81

variables: initial SD concentration, RHB dosage, initial pH and contact time. From Eq. (3), higher initial SD concentration, RHB dosage, and contact time and lower initial pH will result in better SD removals. Table 1 also shows the proximity of the predicted and actual percent SD removals, confirming the reliability of the quadratic model.

The numerical optimization of process parameters achieved a 96% SD removal (predicted) at 100 mg L^{-1} initial SD concentration, 0.5 g of RHB dose and pH 2. At this condition, the residual SD concentration was found at 4 mg L^{-1} and the adsorption capacity was at 3.3 mg g^{-1}. Experimental validation of the model at optimum conditions resulted in 95.5% SD removal, 3.6 mg L^{-1} residual SD concentration and adsorption capacity of 3.4 mg g^{-1}. Based on the percent error (0.52% for SD removal), the model generated is robust and reliable (de Luna et al. 2015).

3.3 Factors affecting SD removal

The effect of initial pH of the water matrix on SD removal is shown in Fig. 4a. The highest SD removals were obtained at pH 2 for both 0.1 and 0.5 g RHB dosages. It is evident from Fig. 4a that SD removal decreased as the solution pH was raised, with the lowest removal observed at pH 7. The pH point-of-zero charge (pH_{pzc}) of RHB is at pH 6.21, as determined by mass titration. At pH 2 ($pH < pH_{pzc}$), the surface of the RHB is positively charged, whereas at pH 7 ($pH > pH_{pzc}$), it is negatively charged (de Luna et al. 2017). Furthermore, SD is an acid and has a dissociation constant (pK_a) value of 4.15. At $pH < pK_a$, the SD molecules are positively charged, while at the $pH > pK_a$, these molecules are negatively charged (de Luna et al. 2017). Thus, at pH 7 where the solution pH was greater than both the adsorbent pH_{pzc} and

Table 2 ANOVA for the response surface model for SD removal using RHB

Source	Sum of squares	*df*	Mean square	*F* value	*p* value Prob > *F*	
Model	7237.57	14	516.97	9.93	< 0.0001	Significant
X_1_initial SD conc. (mg L^{-1})	2107.25	1	2107.25	40.48	< 0.0001	Significant
X_2_RHB dosage (mg)	588.00	1	588.00	11.30	0.0051	Significant
X_3_initial pH	2671.49	1	2671.49	51.32	< 0.0001	Significant
X_4_contact time (min)	571.11	1	571.11	10.97	0.0056	Significant
X_1X_2	127.91	1	127.91	2.46	0.1410	Not significant
X_1X_3	101.48	1	101.48	1.95	0.1860	Not significant
X_1X_4	346.74	1	346.74	6.66	0.0228	Significant
X_2X_3	31.72	1	31.72	0.61	0.4490	Not significant
X_2X_4	64.00	1	64.00	1.23	0.2876	Not significant
X_3X_4	7.61	1	7.61	0.15	0.7084	Not significant
X_1^2	327.81	1	327.81	6.30	0.0261	Significant
X_2^2	168.95	1	168.95	3.25	0.0948	Not significant
X_3^2	1.40	1	1.40	0.027	0.8723	Not significant
X_4^2	239.62	1	239.62	4.60	0.0514	Not significant
Residual	676.69	13	52.05			
Lack of fit	559.67	10	55.97	1.43	0.4252	Not significant
Pure error	117.02	3	39.01			
Cor total	8192.21	29				

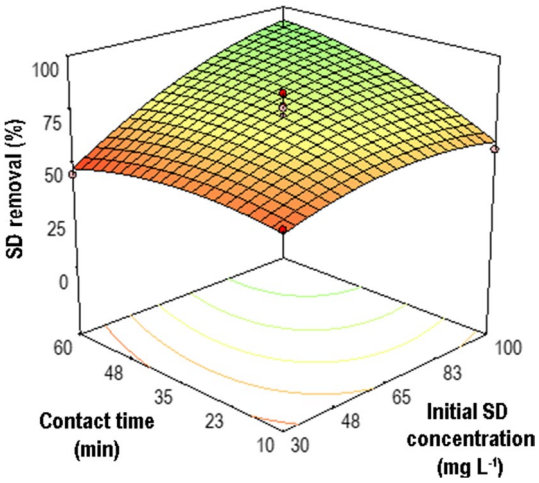

Fig. 3 3D response surface plot of the significant interaction effects of contact time and initial SD concentration on SD removal

the adsorbate pK_a, both RHB and SD had negatively charged surfaces. This explains the low SD removal at higher solution pH, as the increasing electrostatic repulsion reduced the adsorption of SD onto the RHB. When pH is around pK_a of 4.15, the increase of negative species of SD may cause a decrease of removal efficiency. At pH = 2, most of the SD are neutral whereas the adsorbent is positively charged, thus the hydrogen bonding between SD (carbonyl oxygen) and adsorbent (hydroxyl hydrogen) may exist. Also, at lower solution pH, the carboxyl groups (–COOH; $pK_a = 1.7–4.7$) formed negatively charged carboxylate groups ($–COO^-$) (Tran et al. 2017). These adsorbent binding sites were mainly responsible for the high SD removal through interaction with the positively charged SD molecules, even at pH levels below pH_{pzc}. This can be seen from the FTIR results that show large shifts of C = O of carbonyl/carboxyl groups before and after adsorption. For comparison, pH 2 and pH 7 were used in the succeeding experiments.

Figure 4b shows the relationship between SD removal and initial SD concentration (mg L^{-1}) at two different solution pH. As the initial SD concentration was raised from 30 to 100 mg L^{-1} at solution pH of 2, SD removal improved from 88% to 97%. At higher solution pH of 7, SD removals also improved from 61% to 77% for 30 and 100 mg L^{-1} SD solutions, respectively. These indicate that the SD removals are dependent on initial SD concentration. The observed high SD removal at the low initial SD concentration of 30 mg L^{-1}, especially at pH 2, can be attributed to the lower amount of SD molecules competing for sorption onto the RHB surface (Ong et al. 2018). The improved SD removal as the initial SD concentration was raised was due to the increased interaction through collision between the SD molecules and the available binding sites on the RHB, thereby resulting in higher probability of these molecules to attach to the adsorbent (Mane et al. 2007).

Figure 4c shows the relationship between SD removal and RHB dosage. At solution pH of 2 and as RHB

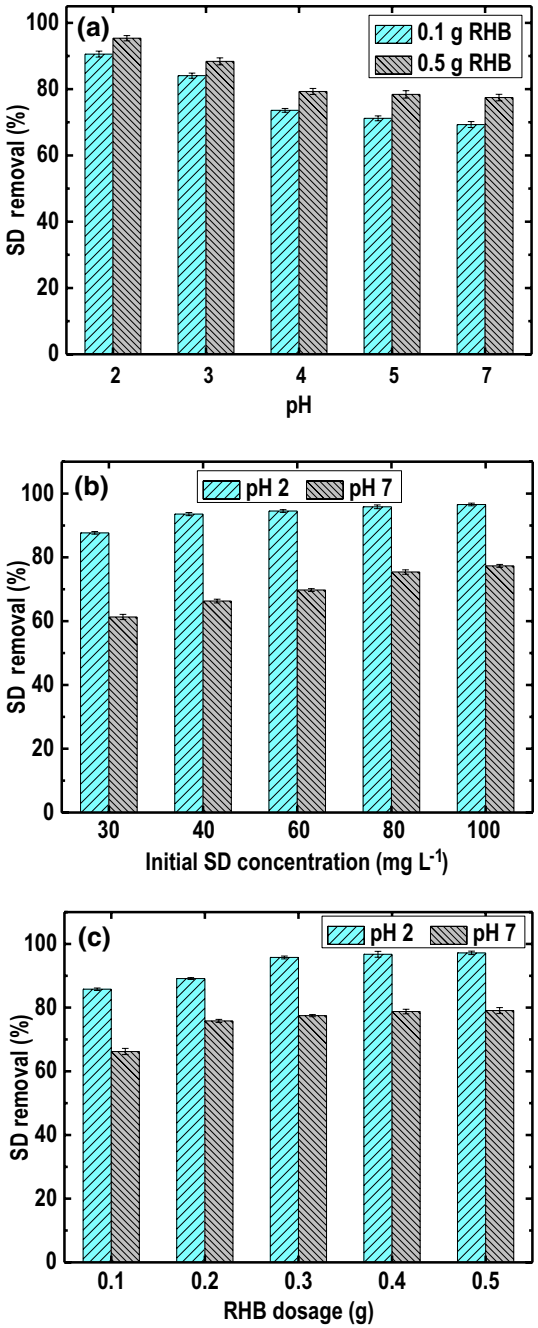

Fig. 4 SD removal at varying **a** initial pH, **b** initial SD concentration, and **c** RHB dosage

dosage increased from 0.1 to 0.5 g, SD removal significantly improved from 86% to 97%. A similar trend was observed at pH 7 where a noticeable rise in SD removal (66–79%) occurred as RHB dosage was increased from 0.1 to 0.5 g. The improvement in SD removal at higher RHB dosage is attributed to the greater number of available binding sites for interaction with SD molecules (Overah 2011).

3.4 Adsorption isotherms

One of the most important criteria in selecting a suitable adsorbent is by studying the adsorption isotherm which provides fundamental physiochemical data for evaluating the adsorption capacities of an adsorbent. The data obtained at the two pH levels were fitted using Langmuir, Freundlich, and Temkin adsorption equations.

The Langmuir isotherm model represents the equilibrium distribution of pollutant molecules between the solid and liquid phases. It is valid for monolayer adsorption onto a surface containing a finite number of identical sites (Langmuir 1918). The model assumes uniform energies of adsorption onto the surface and no transmigration of adsorbate occurs in the plane of the surface. Formation of a monolayer adsorbate on the outer surface of the adsorbent eventually reaches a saturation point where the maximum adsorption of the surface is achieved and no further adsorption takes place (Boparai et al. 2011). Langmuir isotherm model is expressed mathematically in Eq. (4). The values of Q_m and b are computed from the slope and y-intercept of the plot of *1/Q* and *1/Ce*.

$$\frac{1}{Q} = \left[\frac{1}{bQ_m}\right]\frac{1}{C_e} + \frac{1}{Q_m}. \tag{4}$$

The separation factor, R_L, also called the equilibrium parameter, is a dimensionless constant used to validate if experimental data conform to the Langmuir isotherm. The criteria for applicability to the Langmuir isotherm depends on the R_L value as computed using Eq. (5) where: ($R_L = 1$) follows a linear isotherm, ($R_L > 1$) means an unfavorable isotherm, ($R_L < 1$) corresponds to a favorable isotherm, and ($R_L = 0$) is an irreversible isotherm.

$$R_L = \frac{1}{1 + bC_o}. \tag{5}$$

Meanwhile, the Freundlich isotherm assumes heterogeneous surface and adsorption sites with varying energy of adsorption (Freundlich 1906). The model assumes that the stronger binding sites on the heterogeneous surface are initially occupied, and a decrease in binding strength occurs as the degree of site occupation is increased. The Freundlich isotherm can be expressed as follows:

$$\ln Q = \ln K_f + \frac{1}{n}\ln C_e. \tag{6}$$

The slope of *1/n* ranging between 0 and 1 is a measure of adsorption intensity or surface heterogeneity, becoming more heterogeneous as its value approaches zero. A value for *1/n* below one indicates normal Langmuir isotherm.

The Temkin isotherm equation is characterized by a uniform distribution of binding energies (Temkin and Pyzhev 1940). The slope and intercepts are determined by plotting the quantity adsorbed Q against $ln\ C_e$ and the constants and take into account the presence of indirect interactions between the adsorbent and adsorbate as shown in Eq. (7). The model assumes that heat of adsorption (function of temperature) of all molecules in the layer decreases with coverage linearly rather than logarithmically.

$$Q = \beta ln\alpha + \beta lnC_e \tag{7}$$

Shown in Fig. 5 are the plots of the equilibrium adsorption isotherm of diclofenac onto the RHB surface, Langmuir, Freundlich, and Temkin isotherms for initial pH 2 and pH 7, respectively, while Table 3 shows the values for the isotherm parameters. In this study, the Langmuir isotherm gave the highest coefficient of determination for both pH 2 ($R^2 = 0.9827$) and pH 7 ($R^2 = 0.9460$). This indicates that monolayer coverage of SD onto the RHB surface, which contained homogenous and energetically equivalent sites for adsorption, is favored (Ifthikar et al. 2018). Likewise, no transmigration of diclofenac happened in the layer of the RHB surface (de Luna et al. 2013). For the separation factor, R_L, the values ranged from 0.73 to 0.92 at pH 2 and 0.64

Table 3 Isotherm parameters for SD removal using RHB

Parameter	Value	
	pH 2	pH 7
Langmuir		
q_m (mg g^{-1})	14.7929	11.8483
b (L mg^{-1})	0.1703	0.0052
R^2	0.9827	0.9460
Freundlich		
K_f ($mg^{1-1/n}$ $L^{1/n}$ g^{-1})	2.0943	0.0618
n	1.1148	0.9831
R^2	0.9740	0.9258
Temkin		
α (L g^{-1})	2.3621	0.1439
β (J mol^{-1})	2.3458	2.3349
R^2	0.8040	0.8332

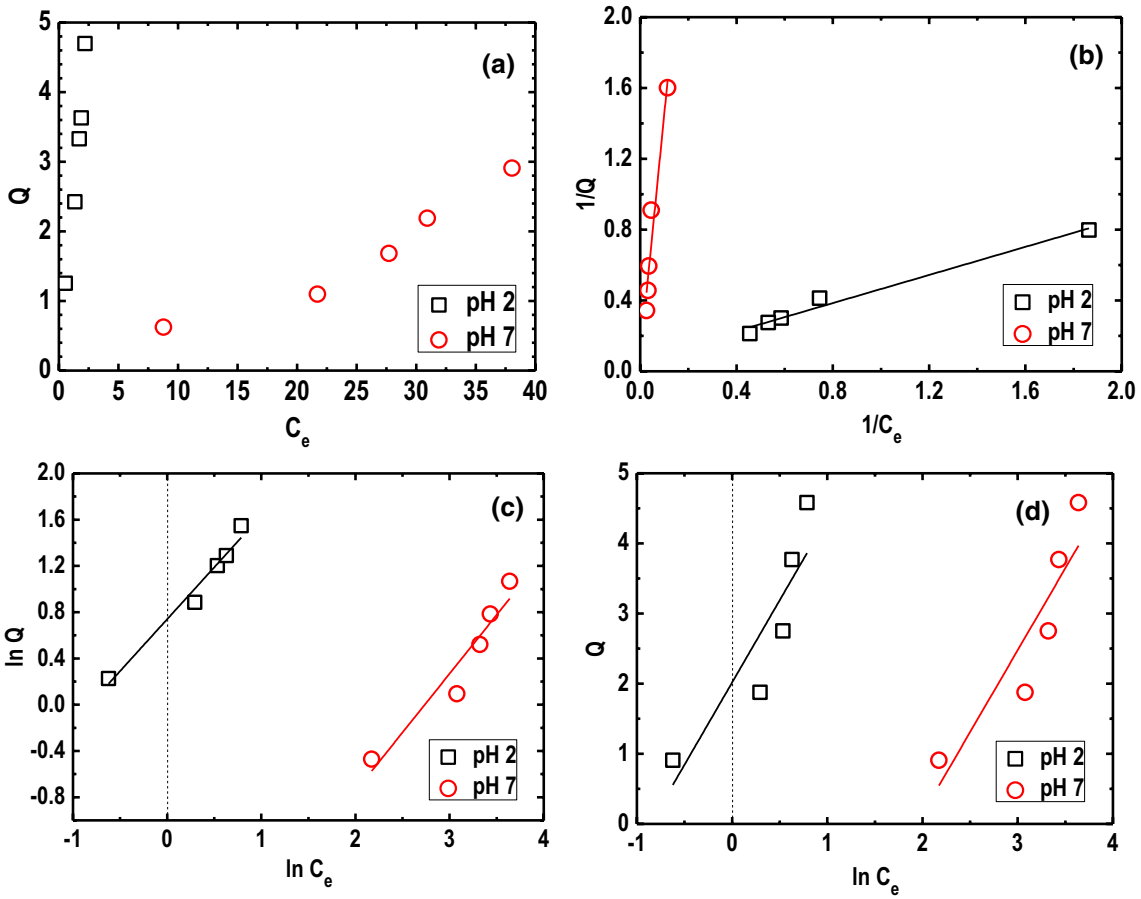

Fig. 5 **a** Adsorption isotherm of SD over RHB, **b** Langmuir, **c** Freundlich and **d** Temkin isotherm plots at pH 2 and pH 7

to 0.89 at pH 7, confirming that the isotherm is favorable at both pH levels. Thus, RHB is a suitable adsorbent for SD.

3.5 Adsorption kinetics

Kinetic modeling was done using pseudo-first-order, pseudo-second-order, and intraparticle diffusion equations for both pH 2 and pH 7 solutions to determine the dominant mechanism that controls the adsorption rate, as shown in Eqs. (8, 9, 10). Pseudo-first-order kinetic model (Lagergren 1898) describes the rate of pollutant removal as directly proportional to the pollutant concentration and assumes physisorption as the rate-controlling mechanism. The integrated linear form of the pseudo-first-order model is shown in the following equation:

$$\log\left(Q - q_t\right) = logQ - \frac{k_1}{2.303}t. \tag{8}$$

On the other hand, the pseudo-second-order kinetic model (Ho and McKay 1998) maintains that the rate of pollutant degradation is directly proportional to the square of pollutant concentration and suggests chemisorption as the rate-controlling step in the adsorption process. This equation indicates the fast decrease in pollutant concentration in the aqueous solution at a short time of contact suggesting an electrostatic interaction. The linearized form of the pseudo-second-order model is shown in the following equation:

$$\frac{t}{q_t} = \frac{1}{k_2 Q^2} + \frac{1}{Q}t. \tag{9}$$

The intraparticle diffusion model describes the transport of the solute from the bulk of the solution onto the adsorbent through an intraparticle process or pore diffusion. The intraparticle diffusion model demonstrating a linear relationship means that the pore diffusion also affects the rate of adsorption. The intraparticle diffusion model is given in the following equation:

$$q_t = k_{id}t^{0.5} + C. \tag{10}$$

If the rate-limiting step is intraparticle diffusion, a plot of solute adsorbed against the square root of the contact time should yield a straight line passing through the origin (Oladoja et al. 2008). However, if the y-intercept, C, is not equal to zero, the mechanism does not uniquely limit the

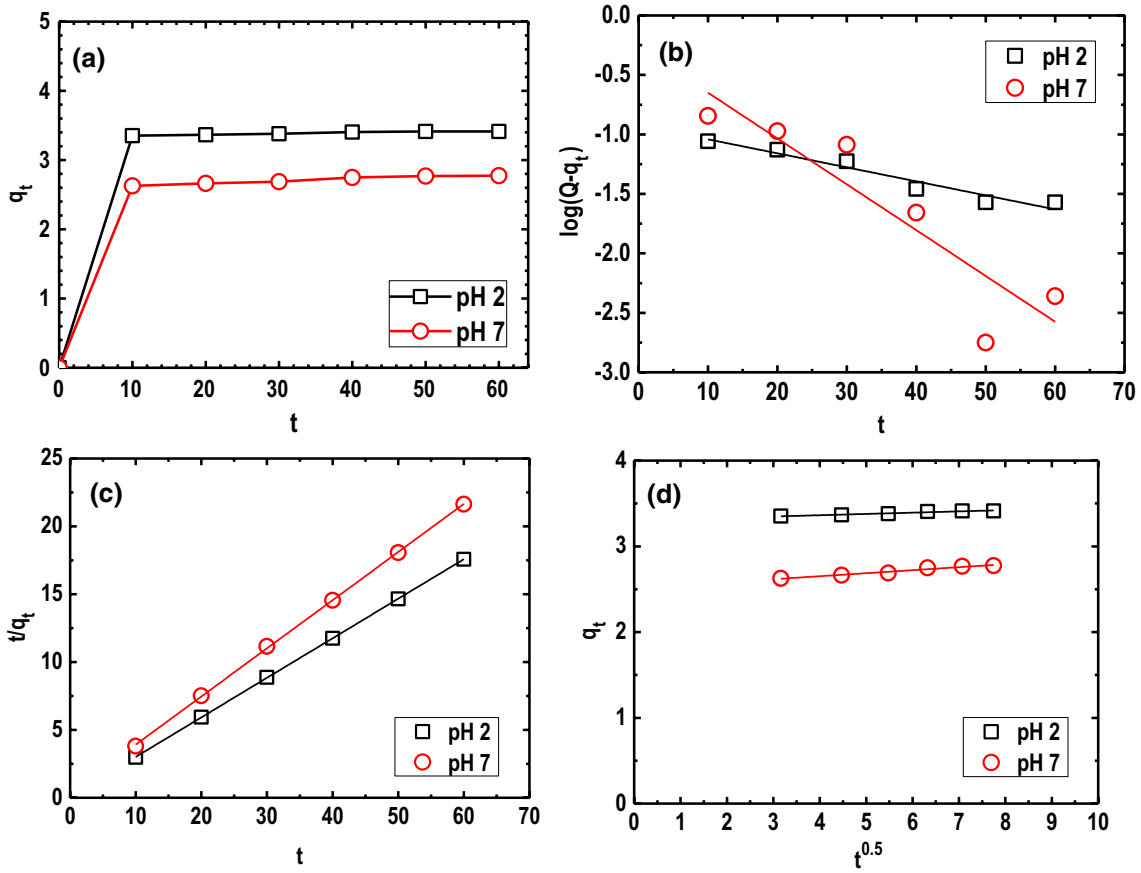

Fig. 6 **a** Effect of contact time, **b** pseudo-first-order **c** pseudo-second-order and **d** intraparticle diffusion kinetic plots at pH 2 and pH 7

Table 4 Kinetic parameters for SD removal by RHB

Parameter	Value	
	pH 2	pH 7
Pseudo-first order		
Q (mg g^{-1})	0.1192	0.5438
k_1 (min^{-1})	0.0272	0.0887
R^2	0.9426	0.8293
Pseudo-second order		
Q (mg g^{-1})	3.4317	2.8193
k_2 (g mg^{-1} min^{-1})	0.8647	0.3393
R^2	0.9999	0.9998
Intraparticle diffusion		
C (mg g^{-1})	3.3033	2.511
k_{id} (mg g^{-1} $min^{-1/2}$)	0.0149	0.0351
R^2	0.9552	0.9651

overall process, but it may be a complex combination of adsorption and intraparticle transport (Cunha et al. 2010).

The kinetic data in Fig. 6a revealed that the adsorption process was fast during the first 10 min, and leveled off immediately afterwards when the adsorption equilibrium was achieved. From Table 4, the pseudo-second-order model provided the best fit, and the plot of t/q_t against t is shown in Fig. 6. This model best described the experimental data as shown by the high coefficients of determination ($R^2 = 0.9999$) for both SD removals at pH 2 and pH 7. This suggests that chemisorption controlled the rate of the adsorption process (Wang et al. 2020a). This mechanism can be described as complexation of the SD molecules with the functional groups present on the RHB, with C=O in the carbonyl or carboxyl groups having the most significant participation as indicated in the large shift of peak attributed to C = O stretching vibrations observed in Fig. 2. As shown in Table 4, the adsorption capacity values ($q_{pH\,2} = 3.4$ and $q_{pH\,7} = 2.8$ mg g^{-1}) determined using regression of the concentration against time were very close to the values ($q_{pH\,2} = 3.4$ and $q_{pH\,7} = 2.3$ mg g^{-1}) obtained during optimization. This renders the pseudo-second-order model more reliable. The value of the pseudo-second-order rate constant, k_2, was higher at pH 2. Thus, SD molecules have high probability of binding to the functional groups on the RHB at low solution pH.

4 Conclusions

The RHB prepared via torrefaction was found effective in removing SD from water matrices. EDX analysis revealed that the elemental composition of the RHB adsorbent surface before and after torrefaction showed an increase in carbon atomic percentage from 25.3% to 40.48%. FTIR spectra for RHB before and after adsorption revealed that C=O stretching vibrations that correspond to the carbonyl or carboxyl groups had major participation in the adsorption process. In the adsorption study, the increase in SD concentration, contact time, and RHB dosage improved SD removal up to 97%, while the increase in the solution pH reduced SD removal. At optimum operating conditions (initial SD concentration = 100 mg L^{-1}, RHB dosage = 0.5 g, pH = 2), SD removal reached 96% and the calculated equilibrium adsorption capacity was 3.3 mg g^{-1}. In addition, the Langmuir isotherm and pseudo-second order kinetics best described SD adsorption on RHB, with the highest coefficients of determination at 0.9827 and 0.9999, respectively. Overall, the biochar adsorbents produced via the torrefaction of rice hulls and in the absence of activating chemicals showed excellent potential for the removal of pharmaceutical compounds such as sodium diclofenac from water matrices.

Acknowledgements The authors would like to thank the Department of Science and Technology, Philippines for providing financial support for this research undertaking.

Author contributions Conceptualization: JQF, MDGDL; methodology: JQF, KKR and SMBPO; investigation: RRMA, KKR and DCO; validation: JQF, SMBPO and RRMA; formal analysis: JQF, RRMA, DCO and SMBPO; resources: MDGDL; data curation: KKR, RRMA, DCO; writing original draft: JQF, KKR, DCO; writing—review and editing: DCO, SMBPO and MDGDL; visualization: RRMA, DCO and KKR; supervision: MDGDL; project administration: MDGDL; funding: MDGDL.

Compliance with ethical standards

Conflict of interest The authors declare no competing financial interest.

References

Abo El Naga AO, El Saied M, Shaban SA, El Kady FY (2019) Fast removal of diclofenac sodium from aqueous solution using sugar cane bagasse-derived activated carbon. J Mol Liq 285:9–19. https://doi.org/10.1016/j.molliq.2019.04.062

Antunes M, Esteves VI, Guégan R, Crespo JS, Fernandes AN, Giovanela M (2012) Removal of diclofenac sodium from aqueous solution by Isabel grape bagasse. Chem Eng J 192:114–121. https://doi.org/10.1016/j.cej.2012.03.062

Arpia AA, Chen WH, Lam SS, Rousset P, de Luna MDG (2021) Sustainable biofuel and bioenergy production from biomass waste residues using microwave-assisted heating: a comprehensive review. Chem Eng J 403:126233. https://doi.org/10.1016/j.cej.2020.126233

Arriola E, Chen WH, Chih YK, De Luna MD, Show PL (2020) Impact of post-torrefaction process on biochar formation from wood pellets and self-heating phenomena for production safety. Energy 207:118324. https://doi.org/10.1016/j.energy.2020.118324

Boparai HK, Joseph M, O'Carroll DM (2011) Kinetics and thermodynamics of cadmium ion removal by adsorption onto nano

zerovalent iron particles. J Hazard Mater 186:458–465. https://doi.org/10.1016/j.jhazmat.2010.11.029

Chen H, Wang H, Xue Z, Yang L, Xiao Y, Zheng M, Lei B, Liu Y, Sun L (2012) High hydrogen storage capacity of rice hull based porous carbon. Int J Hydrog Energy 37:18888–18894. https://doi.org/10.1016/j.ijhydene.2012.09.035

Coates J (2000) Interpretation of infrared spectra, a practical approach. In: Meyers RA (ed) Encyclopedia of analytical chemistry. John Wiley and Sons Ltd, Chichester, pp 10815–10837

da Cunha GC, Romão LPC, Santos MC, Araújo BR, Navickiene S, de Pádua VL (2010) Adsorption of trihalomethanes by humin: batch and fixed bed column studies. Bioresour Technol 101:3345–3354. https://doi.org/10.1016/j.biortech.2009.11.096

de Luna MDG, Veciana ML, Su C-C, Lu M-C (2012) Acetaminophen degradation by electro-Fenton and photoelectro-Fenton using a double cathode electrochemical cell. J Hazard Mater 217:200–207. https://doi.org/10.1016/j.jhazmat.2012.03.018

de Luna MDG, Flores ED, Genuino DAD, Futalan CM, Wan MW (2013) Adsorption of Eriochrome Black T (EBT) dye using activated carbon prepared from waste rice hulls-Optimization, isotherm and kinetic studies. J Taiwan Inst Chem Eng 44:646–653. https://doi.org/10.1016/j.jtice.2013.01.010

de Luna MDG, Abarca RRM, Su C-C, Huang Y-H, Lu M-C (2015) Multivariate optimization of phosphate removal and recovery from aqueous solution by struvite crystallization in a fluidized-bed reactor. Desalin Water Treat 55:496–505. https://doi.org/10.1080/19443994.2014.915584

de Luna MDG, Murniati BW, Rivera KKP, Arazo RO (2017) Removal of sodium diclofenac from aqueous solution by adsorbents derived from cocoa pod husks. J Environ Chem Eng 5:1465–1474. https://doi.org/10.1016/J.JECE.2017.02.018

de Luna MDG, Paragas LKB, Doong R-A (2019) Insights into the rapid elimination of antibiotics from aqueous media by tunable C_3N_4 photocatalysts: effects of dopant amount, co-existing ions and reactive oxygen species. Sci Total Environ 669:1053–1061. https://doi.org/10.1016/J.SCITOTENV.2019.03.003

de Souza MF, Magalhães WLE, Persegil MC (2002) Silica derived from burned rice hulls. Mater Res 5:467–474. https://doi.org/10.1590/S1516-14392002000400012

Ensano B, Borea L, Naddeo V, Belgiorno V, de Luna M, Ballesteros F (2017) Removal of pharmaceuticals from wastewater by intermittent electrocoagulation. Water 9:85. https://doi.org/10.3390/w9020085

Fei XW, Liu LY, Xu JG, Zhang ZH, Mei YA (2006) The non-steroidal anti-inflammatory drug, diclofenac, inhibits Na^+ current in rat myoblasts. Biochem Biophys Res Commun 346:1275–1283. https://doi.org/10.1016/j.bbrc.2006.06.034

Freundlich H (1906) Über die Adsorption in Lösungen. Zeitschrift für Phys Chemie 57:385–470. https://doi.org/10.1515/zpch-1907-5723

Genuino DAD, Bataller BG, Capareda SC, de Luna MDG (2017) Application of artificial neural network in the modeling and optimization of humic acid extraction from municipal solid waste biochar. J Environ Chem Eng 5:4101–4107. https://doi.org/10.1016/J.JECE.2017.07.071

Genuino DAD, de Luna MDG, Capareda SC (2018) Improving the surface properties of municipal solid waste-derived pyrolysis biochar by chemical and thermal activation: optimization of process parameters and environmental application. Waste Manag 72:255–264. https://doi.org/10.1016/J.WASMAN.2017.11.038

Gotostos MJN, Su C, LunaLu MGGM (2014) Kinetic study of acetaminophen degradation by visible light photocatalysis. J Environ Sci Heal Part A 49:892–899. https://doi.org/10.1080/10934529.2014.894310

Green RE, Newton I, Shultz S, Cunningham AA, Gilbert M, Pain DJ, Prakash V (2004) Diclofenac poisoning as a cause of vulture population declines across the Indian subcontinent. J Appl Ecol 41:793–800. https://doi.org/10.1111/j.0021-8901.2004.00954.x

Han TU, Kim J, Kim K (2020) Freezing-accelerated removal of chromate by biochar synthesized from waste rice husk. Sep Purif Technol 250:117233. https://doi.org/10.1016/j.seppur.2020.117233

Ho YS, McKay G (1998) A Comparison of chemisorption kinetic models applied to pollutant removal on various sorbents. Process Saf Environ Prot 76:332–340. https://doi.org/10.1205/095758298529696

Hu X, Yang J, Zhang J (2011) Magnetic loading of $TiO_2/SiO_2/Fe_3O_4$ nanoparticles on electrode surface for photoelectrocatalytic degradation of diclofenac. J Hazard Mater 196:220–227. https://doi.org/10.1016/j.jhazmat.2011.09.009

Ifthikar J, Wang T, Khan A, Jawad A, Sun T, Jiao X, Chen Z, Wang J, Wang Q, Wang H, Jawad A (2017) Highly efficient lead distribution by magnetic sewage sludge biochar: sorption mechanisms and bench applications. Bioresour Technol 238:399–406. https://doi.org/10.1016/j.biortech.2017.03.133

Ifthikar J, Jiao X, Ngambia A, Wang T, Khan A, Jawad A, Xue Q, Liu L, Chen Z (2018) Facile one-pot synthesis of sustainable carboxymethyl chitosan – sewage sludge biochar for effective heavy metal chelation and regeneration. Bioresour Technol 262:22–31. https://doi.org/10.1016/j.biortech.2018.04.053

Jeon C (2011) Removal of copper ion using rice hulls. J Ind Eng Chem 17:517–520. https://doi.org/10.1016/j.jiec.2010.10.020

Kalderis D, Bethanis S, Paraskeva P, Diamadopoulos E (2008) Production of activated carbon from bagasse and rice husk by a single-stage chemical activation method at low retention times. Bioresour Technol 99:6809–6816. https://doi.org/10.1016/j.biortech.2008.01.041

Khan N, Chowdhary P, Ahmad A, Shekher Giri B, Chaturvedi P (2020) Hydrothermal liquefaction of rice husk and cow dung in Mixed-Bed-Rotating Pyrolyzer and application of biochar for dye removal. Bioresour Technol 309:123294. https://doi.org/10.1016/j.biortech.2020.123294

Kim DG, Choi D, Cheon S, Ko SO, Kang S, Oh S (2020) Addition of biochar into activated sludge improves removal of antibiotic ciprofloxacin. J Water Process Eng. https://doi.org/10.1016/j.jwpe.2019.101019

Lagergren S (1898) Zur theorie der sogenannten adsorption geloster stoffe (About the theory of so-called adsorption of soluble substances). K Sven Vetenskapsakademiens Handlingar 24:1–39

Langmuir I (1918) The adsorption of gases on plane surfaces of glass, mica and platinum. J Am Chem Soc 40:1361–1403. https://doi.org/10.1021/ja02242a004

Leksungnoen P, Wisawapipat W, Ketrot D, Aramrak S, Nookabkaew S, Rangkadilok N, Satayavivad J (2019) Biochar and ash derived from silicon-rich rice husk decrease inorganic arsenic species in rice grain. Sci Total Environ 684:360–370. https://doi.org/10.1016/j.scitotenv.2019.05.247

Lim JS, Abdul Manan Z, Wan Alwi SR, Hashim H (2012) A review on utilisation of biomass from rice industry as a source of renewable energy. Renew Sustain Energy Rev 16:3084–3094. https://doi.org/10.1016/j.rser.2012.02.051

Lin JC-T, de Luna MDG, Aranzamendez GL, Lu M-C (2016) Degradations of acetaminophen via a $K_2S_2O_8$-doped TiO_2 photocatalyst under visible light irradiation. Chemosphere 155:388–394. https://doi.org/10.1016/J.CHEMOSPHERE.2016.04.059

Liu J-L, Wong M-H (2013) Pharmaceuticals and personal care products (PPCPs): a review on environmental contamination in China. Environ Int 59:208–224. https://doi.org/10.1016/j.envint.2013.06.012

Malefane ME, Feleni U, Kuvarega AT (2019) Cobalt (II/III) oxide and tungsten (VI) oxide p-n heterojunction photocatalyst for photodegradation of diclofenac sodium under visible light. J Environ Chem Eng. https://doi.org/10.1016/j.jece.2019.103560

Mane VS, Deo Mall I, Chandra Srivastava V (2007) Kinetic and equilibrium isotherm studies for the adsorptive removal of Brilliant Green dye from aqueous solution by rice husk ash. J Environ Manag 84:390–400. https://doi.org/10.1016/j.jenvman.2006.06.024

Martínez C, Canle LM, Fernández MI, Santaballa JA, Faria J (2011) Aqueous degradation of diclofenac by heterogeneous photocatalysis using nanostructured materials. Appl Catal B Environ 107:110–118. https://doi.org/10.1016/j.apcatb.2011.07.003

Matin AA, Farajzadeh MA, Jouyban A (2005) A simple spectrophotometric method for determination of sodium diclofenac in pharmaceutical formulations. Farmaco 60:855–858. https://doi.org/10.1016/j.farmac.2005.05.011

Nakbanpote W, Thiravetyan P, Kalambaheti C (2000) Preconcentration of gold by rice husk ash. Miner Eng 13:391–400. https://doi.org/10.1016/S0892-6875(00)00021-2

Oaks JL, Gilbert M, Virani MZ, Watson RT, Meteyer CU, Rideout BA, Shivaprasad HL, Ahmed S, Chaudhry MJI, Arshad M, Mahmood S, Ali A, Khan AA (2004) Diclofenac residues as the cause of vulture population decline in Pakistan. Nature 427:630–633. https://doi.org/10.1038/nature02317

Oladoja NA, Aboluwoye CO, Oladimeji YB (2008) Kinetics and isotherm studies on Methylene Blue adsorption onto ground palm kernel coat. Turk J Eng Environ Sci 32:303–312

Ong DC, Pingul-Ong SMB, Kan CC, de Luna MDG (2018) Removal of nickel ions from aqueous solutions by manganese dioxide derived from groundwater treatment sludge. J Clean Prod 190:443–451. https://doi.org/10.1016/j.jclepro.2018.04.175

Overah L (2011) Biosorption of Cr (III) from aqueous solution by the leaf biomass of *Calotropis procera*–'*Bom bom*'. J Appl Sci Environ Manag 15:87–95. https://doi.org/10.4314/jasem.v15i1.65681

Paragas LKB, de Luna MDG, Doong R-A (2018) Rapid removal of sulfamethoxazole from simulated water matrix by visible-light responsive iodine and potassium co-doped graphitic carbon nitride photocatalysts. Chemosphere 210:1099–1107. https://doi.org/10.1016/J.CHEMOSPHERE.2018.07.109

Shi J, Fan X, Tsang DCW, Wang F, Shen Z, Hou D, Alessi DS (2019) Removal of lead by rice husk biochars produced at different temperatures and implications for their environmental utilizations. Chemosphere 235:825–831. https://doi.org/10.1016/j.chemosphere.2019.06.237

Sotelo JL, Rodríguez A, Álvarez S, García J (2012) Removal of caffeine and diclofenac on activated carbon in fixed bed column. Chem Eng Res Des 90:967–974. https://doi.org/10.1016/j.cherd.2011.10.012

Stülten D, Zühlke S, Lamshöft M, Spiteller M (2008) Occurrence of diclofenac and selected metabolites in sewage effluents. Sci Total Environ 405:310–316. https://doi.org/10.1016/j.scitotenv.2008.05.036

Sumalinog DAG, Capareda SC, de Luna MDG (2018) Evaluation of the effectiveness and mechanisms of acetaminophen and methylene blue dye adsorption on activated biochar derived from municipal solid wastes. J Environ Manag 210:255–262. https://doi.org/10.1016/J.JENVMAN.2018.01.010

Temkin MI, Pyzhev V (1940) Kinetics of ammonia synthesis on promoted iron catalyst. Acta Physicochim 12:327–356

Tiwari D, Lalhriatpuia C, Lee SM (2015) Hybrid materials in the removal of diclofenac sodium from aqueous solutions: batch and column studies. J Ind Eng Chem 30:167–173. https://doi.org/10.1016/j.jiec.2015.05.018

Tran HN, You S-J, Hosseini-Bandegharaei A, Chao H-P (2017) Mistakes and inconsistencies regarding adsorption of contaminants from aqueous solutions: a critical review. Water Res 120:88–116. https://doi.org/10.1016/J.WATRES.2017.04.014

Wang D, Sakoda A, Suzuki M (2001) Biological efficiency and nutritional value of Pleurotus ostreatus cultivated on spent beer grain. Bioresour Technol 78:293–300. https://doi.org/10.1016/S0960-8524(01)00002-5

Wang H, Liu Y, Ifthikar J, Shi L, Khan A, Chen Z, Chen Z (2018) Towards a better understanding on mercury adsorption by magnetic bio-adsorbents with Γ-Fe2O3 from pinewood sawdust derived hydrochar: influence of atmosphere in heat treatment. Bioresour Technol 256:269–276. https://doi.org/10.1016/j.biortech.2018.02.019

Wang H, Wang S, Chen Z, Zhou X, Wang J, Chen Z (2020a) Engineered biochar with anisotropic layered double hydroxide nanosheets to simultaneously and efficiently capture Pb2+ and CrO42− from electroplating wastewater. Bioresour Technol 306:123118. https://doi.org/10.1016/j.biortech.2020.123118

Wang L, Bolan NS, Tsang DCW, Hou D (2020b) Green immobilization of toxic metals using alkaline enhanced rice husk biochar: effects of pyrolysis temperature and KOH concentration. Sci Total Environ 720:137584. https://doi.org/10.1016/j.scitotenv.2020.137584

Wu L, Du C, He J, Yang Z, Li H (2019) Effective adsorption of diclofenac sodium from neutral aqueous solution by low-cost lignite activated cokes. J Hazard Mater. https://doi.org/10.1016/j.jhazmat.2019.121284

Yu GX, Jin M, Sun J, Zhou XL, Chen LF, Wang JA (2013) Oxidative modifications of rice hull-based carbons for dibenzothiophene adsorptive removal. Catal Today 212:31–37. https://doi.org/10.1016/j.cattod.2012.09.020